Available online at www.sciencedirect.com

SCIENCE DIRECT

Vision Research 46 (2006) 1574–1584

Vision Research

www.elsevier.com/locate/visres

Contrast sensitivity for letter optotypes vs. gratings under conditions biased toward parvocellular and magnocellular pathways

J. Jason McAnany [a], Kenneth R. Alexander [a,b,*]

[a] Department of Psychology, University of Illinois at Chicago, 1007 W. Harrison Street, Chicago, IL 60612, USA

[b] Department of Ophthalmology and Visual Sciences, University of Illinois at Chicago, 1855 W. Taylor Street, Chicago, IL 60612, USA

Received 18 April 2005; received in revised form 26 July 2005

Abstract

This study examined the extent to which letter optotypes and grating stimuli provide equivalent measures of contrast sensitivity under conditions designed to favor the magnocellular (MC) and parvocellular (PC) pathways. The contrast sensitivity functions (CSFs) of three visually normal observers were measured for Sloan letters and Gabor patches, using steady- and pulsed-pedestal paradigms to bias processing toward MC and PC pathways, respectively. CSFs for Gabor patches were low-pass for the steady-pedestal paradigm and band-pass for the pulsed-pedestal paradigm, in agreement with previous reports. However, CSFs for letters were low-pass for both testing paradigms. CSFs for letters restricted in frequency content by spatial filtering were equivalent to those for Gabor patches for both testing paradigms. Results indicate that conventional letter optotypes can provide a misleading measure of contrast sensitivity, especially under conditions emphasizing the PC pathway. The use of spatially band-pass filtered letters can provide a more appropriate evaluation of spatial contrast sensitivity while maintaining some of the potential advantages of letters.

Keywords: Contrast sensitivity; Letters; Magnocellular; Parvocellular

1. Introduction

The measurement of spatial contrast sensitivity has often been used in the clinical setting, typically in conjunction with an assessment of visual acuity, to gain information regarding visual dysfunction in ocular diseases. Two general classes of test stimuli have been used to measure contrast sensitivity: gratings and letter optotypes. Grating stimuli are appropriate for isolating the low-level analyzers that are thought to underlie pattern vision (Graham, 1989). However, letters may have several practical advantages over gratings in the clinical evaluation of visual function. For example, letters are less susceptible to the spurious resolution and spatial aliasing that can occur with periodic stimuli such as gratings (e.g., Herse & Bedell, 1989; Wang, Bradley, & Thibos, 1997). In addition, letters are familiar to patients, they are easily incorporated into a psychophysical paradigm, and like stimuli in the natural environment, letters contain a broad range of spatial frequencies at different orientations (Pelli, Robson, & Wilkins, 1988; Regan, 1991). However, a fundamental unresolved question is the extent to which letters and gratings provide equivalent information about spatial contrast sensitivity, particularly within the context of magnocellular (MC) and parvocellular (PC) pathways.

It is generally held that contrast encoding within the visual system is mediated by two processing streams, the MC and PC pathways, with different response properties (Kaplan, Lee, & Shapley, 1990; Lee, 1996; Merigan & Maunsell, 1993). At the level of the retina and lateral geniculate nucleus (LGN), the MC pathway has a high contrast gain and approaches saturation at relatively low levels of contrast. The PC pathway has a more linear contrast response function that extends to high contrast levels. It is presumed that the MC pathway is involved in the detection

* Corresponding author. Tel.: +1 312 996 5825; fax: +1 312 996 7770.
E-mail address: kennalex@uic.edu (K.R. Alexander).

0042-6989/$ - see front matter © 2005 Elsevier Ltd. All rights reserved.
doi:10.1016/j.visres.2005.08.019

and discrimination of briefly presented, achromatic patterns of low contrast, whereas the PC pathway is thought to mediate visual resolution and chromatic processing (reviewed by Lennie, 1993).

Recently, steady-pedestal and pulsed-pedestal paradigms have been introduced to assess the spatial contrast sensitivity of the MC and PC pathways, respectively (Leonova, Pokorny, & Smith, 2003). The steady-pedestal paradigm consists of the brief presentation of a test stimulus against a continuously presented luminance pedestal. This paradigm is thought to favor the MC pathway, at least at low to intermediate spatial frequencies and large target sizes, because the test target is presented only briefly. The pulsed-pedestal paradigm consists of the simultaneous brief presentation of a test stimulus and luminance pedestal. This paradigm is thought to favor the PC pathway because the abrupt onset of the luminance pedestal drives the MC pathway toward saturation. Psychophysical data acquired using these two paradigms have the contrast response properties and temporal summation characteristics associated with the MC and PC pathways described electrophysiologically, as discussed previously (Leonova et al., 2003; Pokorny & Smith, 1997).

Spatial contrast sensitivity functions (CSFs) for grating stimuli obtained using the steady-pedestal and pulsed-pedestal paradigms differ substantially in shape (Leonova et al., 2003). For the steady-pedestal paradigm, the CSF is typically low-pass, similar to the results of previous studies that targeted "transient" visual mechanisms (e.g., Kulikowski & Tolhurst, 1973; Legge, 1978; Wilson, 1980). For the pulsed-pedestal paradigm, the CSF is typically more band-pass in shape, similar to results obtained when "sustained" visual mechanisms are emphasized (e.g., Chung, Legge, & Tjan, 2002; Legge, 1978; Wilson, 1980; Rohaly & Owsley, 1993). As a result, the greatest difference in contrast sensitivity between the steady- and pulsed-pedestal paradigms occurs at the lowest spatial frequencies, and the CSFs for the two paradigms tend to converge at high spatial frequencies. At intermediate and low spatial frequencies, contrast sensitivity is presumed to be mediated by the MC pathway for the steady-pedestal paradigm and by the PC pathway for the pulsed-pedestal paradigm (Leonova et al., 2003). The convergence of the CSFs for the two paradigms at high spatial frequencies has been attributed to the mediation of contrast sensitivity by the PC pathway for both paradigms.

The CSF for letter optotypes is typically low-pass in shape (Alexander, Derlacki, & Fishman, 1992; Majaj, Pelli, Kurshan, & Palomares, 2002), similar to the results obtained with grating stimuli under conditions that favor the MC pathway. This similarity suggests that the MC pathway may mediate letter contrast sensitivity. However, contrast sensitivity measurements using letter optotypes are typically obtained with relatively long viewing durations. With extended viewing, contrast sensitivities can be equivalent for stimulus conditions that emphasize the MC and PC pathways (Pokorny & Smith, 1997), so either pathway could potentially mediate performance. Further, when the duration of letter presentation is varied explicitly, the critical duration for temporal integration is quite long (Alexander, Derlacki, Fishman, & Szlyk, 1993). This finding is more consistent with letter identification being mediated by the PC pathway, which has a longer critical duration than the MC pathway (Pokorny & Smith, 1997). Therefore, it is presently unclear whether contrast sensitivity for letter identification is mediated by the MC or the PC pathway, and whether the results depend on the stimulus presentation characteristics.

The aim of the present study was to clarify the nature of the visual processes that govern letter contrast sensitivity by measuring the CSF for letter optotypes under conditions designed to favor either the MC or the PC pathway. Experiment 1 compared CSFs for letter optotypes with those for Gaussian-windowed sinewave gratings (Gabor patches), using the steady- and pulsed-pedestal paradigms of Leonova et al. (2003). The purpose was to determine the extent to which the CSF for letter optotypes is similar in shape to that for grating stimuli under conditions that favor the MC and PC pathways. In Experiment 2, increment thresholds were measured as a function of pedestal luminance for Sloan letters and Gabor patches of an intermediate size/spatial frequency, using the steady-pedestal and pulsed-pedestal paradigms. Leonova et al. (2003) showed that the shape of the increment threshold function differs substantially for these two paradigms, which provides an additional way to infer the identity of the pathway that mediates contrast sensitivity. Experiment 3 measured CSFs under the steady- and pulsed-pedestal paradigms for letter stimuli that were restricted in frequency content by spatial filtering with a cosine log filter (Peli, 1990). The CSFs for filtered letters were compared to those for Gabor patches of corresponding spatial frequencies to determine the manner in which the broad spatial frequency content of letters may affect the letter CSF under conditions favoring the MC and PC pathways.

2. Methods

2.1. Subjects

Three subjects with normal best-corrected visual acuity participated in the study. Subjects S1 and S2, male, ages 59 and 25 year, respectively, are the two authors, and participated in all experiments described. Subject S1 has mild deuteranomaly and subject S2 has normal color vision, as assessed with an anomaloscope. Subject S3, female, age 28 yr, with normal color vision, is an experienced psychophysical observer who was naïve as to the purpose of the research. S3 participated in Experiments 1 and 3. Appropriate institutional review board approval was obtained, and subjects gave informed consent before testing.

2.2. Instrumentation

Stimuli were generated by a Macintosh G4 computer and were displayed on an NEC monitor (FE2111SB) with a resolution of 1280×1024 and an 85-Hz refresh rate, driven by an ATI Radeon video card (9000 Pro) with 10-bit resolution. The monitor, which was the only source of illumination in the room, was viewed monocularly from 1.75 m through a phoroptor with the subject's best refractive correction. Experiments were written in Matlab using the Psychophysics Toolbox extensions (Brainard, 1997).

2.3. Stimuli and testing paradigms

Three types of test stimuli were used: Gabor patches, Sloan letters, and spatially band-pass-filtered Sloan letters. Each Gabor patch consisted of a sinewave grating multiplied by a circular Gaussian window whose space constant was proportional to the grating period such that the Gabor patches had a constant number of cycles (3) across spatial frequency. The peak spatial frequency of the Gabor patches ranged from 0.36 to 8.8 cycles per degree (cpd) in approximately 0.3 log unit steps, and the width of the corresponding circular Gaussian windows ranged from 8.3° to 0.34° of visual angle. The Gabor patches were presented in sine phase and had a spatial frequency bandwidth of approximately one octave at half-height. An example of a Gabor patch is presented in Fig. 1 (top).

The Sloan letter set consisted of 10 letters (C, D, H, K, N, O, R, S, V, Z) constructed according to standard guidelines (National Academy of Sciences, 1980). An illustration of a Sloan letter is presented in Fig. 1 (middle). The letters ranged from 0.3 to 1.9 log MAR (minimum angle of resolution) in approximately 0.3 log unit steps. The Sloan letter sizes were chosen to correspond approximately to the peak spatial frequencies of the Gabor patches, based on the standard assumption that 0.0 log MAR (20/20 Snellen equivalent) corresponds to 30 cpd (Regan, Raymond, Ginsburg, & Murray, 1981). As per the NAS guidelines (1980), the stroke width of the letters was 1/5 the letter width, so that there were effectively 2.5 cycles per letter (cpl). As seen in Fig. 1, the spatial extent of the letters was approximately equal to that of the Gabor patches.

A set of frequency-limited Sloan letters was constructed by filtering the original letters with a cosine log filter (Peli, 1990). The cosine log filter, with a center frequency of 2^i cycles per picture, is expressed as

$$G_i(r) = 1/2[1 + \cos(\pi \log_2 r - i\pi)], \quad (1)$$

where $r = \sqrt{u^2 + v^2}$, and u and v are the horizontal and vertical spatial frequency coordinates, respectively. As discussed elsewhere (Peli, 1990), the cosine log filter has the following characteristics: (1) the filter is symmetrical on a log spatial frequency axis; (2) the two-dimensional filter is torus-shaped in the frequency domain; and (3) the bandwidth at half-height is one octave. Thus, the spatial frequency bandwidth of the filtered letters was similar to that of the Gabor patches. The peak object frequency of the filter was set to a constant 2.5 cpl. This is the object frequency of maximum sensitivity for large letters (Alexander, Xie, & Derlacki, 1994; Chung et al., 2002), and, as noted above, it is the object frequency corresponding to Sloan

Fig. 1. Illustration of the test stimuli: Gabor patch (top); Sloan letter (middle); Sloan letter filtered with a cosine log filter centered at 2.5 cycles per letter (bottom).

letter stroke width. This object frequency also produces the highest root mean square (RMS) contrast energy of Sloan letters when they are filtered with a cosine log filter across a range of center frequencies. An illustration of a Sloan letter filtered with the cosine log filter is given in Fig. 1 (bottom).

As shown in Fig. 2, the test targets were presented in the center of a luminance pedestal that subtended 11.1° horizontally and 9.2° vertically. The pedestal in turn was presented in the center of a surround whose outer edges subtended 11.9° horizontally and 9.6° vertically. To aid fixation, four diagonal black lines that extended from the edges of the pedestal to a region just outside the test stimulus were presented continuously.

The two testing paradigms of Leonova et al. (2003) were used, as illustrated in Fig. 2. For the steady-pedestal paradigm (Fig. 2, top), the luminance pedestal was presented continuously in the center of the surround. During the test period, the test target was presented briefly in the center of the pedestal. For the pulsed-pedestal paradigm (Fig. 2, bottom), the pedestal initially had a luminance equal to that of the surround. During the test period, the pedestal was incremented (or decremented) briefly in luminance, and the test target was presented simultaneously with the pedestal. For both testing paradigms, the stimulus duration was 35 ms (3 video frames). The temporal characteristics of the stimuli were confirmed using an oscilloscope and photocell.

Sloan letter contrast (C_l) was defined as Weber contrast, as per convention

$$C_l = (L_t - L_p)/L_p, \quad (2)$$

where L_t is the luminance of the test letter, and L_p is the pedestal luminance. All letters were of positive contrast (i.e., letter luminance was higher than pedestal luminance). Clinical letter charts typically use letters of negative contrast, but, as demonstrated previously (Alexander, Xie, & Derlacki, 1993), CSFs are identical for letters of positive and negative contrast polarity when contrast is defined by the Weber definition. The contrast of the Gabor patches (C_g) was defined similarly as

$$C_g = (L_{max} - L_p)/L_p, \quad (3)$$

where L_{max} is the maximum luminance of the Gabor patch. An equivalent contrast definition was used in previous studies that employed D6 patterns (sixth spatial derivatives of Gaussians) as test stimuli (e.g., Leonova et al., 2003; Swanson & Wilson, 1985), and it was used here to allow a comparison to the results for letter optotypes. In Experiments 1 and 3, L_p was 60 cd/m^2. In Experiment 2, the values of L_p were 15, 19, 24, 30, 38, 48, and 60 cd/m^2. The surround luminance was maintained at 30 cd/m^2 for all conditions. The display luminances were calibrated with a Minolta LS-110 photometer.

A relative definition of contrast was used to describe the filtered letters (Alexander et al., 1994; Chung et al., 2002), because the contrast of complex images is difficult to define (Peli, 1990). The contrast of the filtered letters was defined relative to the original letters from which they were derived, without rescaling. For example, if the contrast value of the original letter was 1.0, the filtered image was assigned a contrast of 1.0, regardless of the actual spatial distribution of the luminance values in the image.

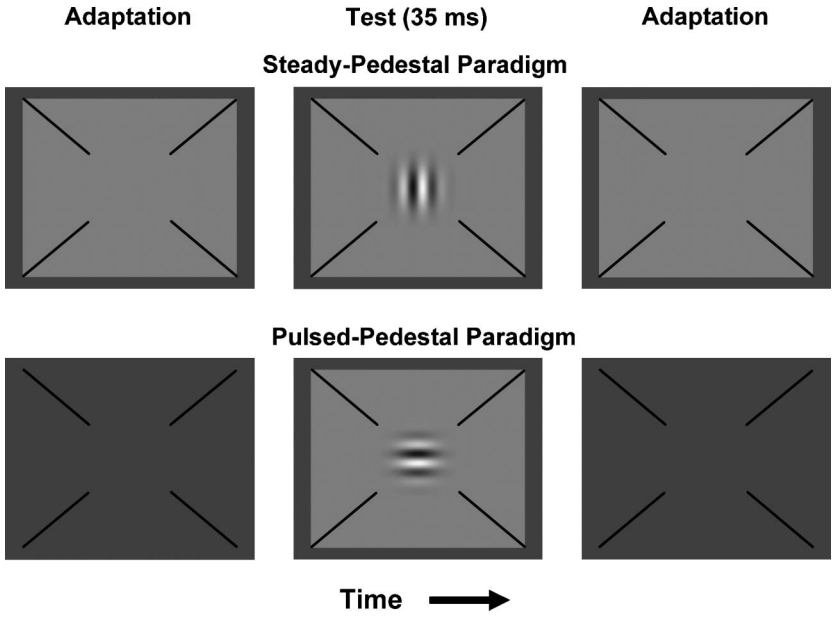

Fig. 2. Illustration of the stimulus display. For the steady-pedestal paradigm (top), a pedestal was presented continuously in the center of a constant surround during the adaptation period. During the test interval, the test stimulus (represented here by a Gabor patch) was presented briefly in the center of the luminance pedestal. For the pulsed-pedestal paradigm (bottom), the pedestal was equal in luminance to the surround luminance during the adaptation period. During the test interval, the pedestal was incremented (or decremented) briefly in luminance, with the test target presented simultaneously in the center of the pedestal. For both paradigms, 4 fixation guides (diagonal lines), which terminated just outside the region of the test stimulus, were shown continuously. The test interval was 35 ms for both paradigms.

2.4. Procedure

A 30-s adaptation period preceded each testing condition, and a brief warning tone signaled the start of each test stimulus presentation. For Gabor patches, the task was to determine the orientation, which was randomly horizontal or vertical on each trial. For letters, the task was to identify the letter that was presented, which was chosen randomly from the set of 10 on each trial. No feedback was given. Each testing session employed a single type of test target. Sessions were ordered in a pseudo-random sequence, and each session was presented 3 times. For Experiment 1, there were 6 Gabor peak spatial frequencies and 7 letter sizes, each presented according to the steady- and pulsed-pedestal paradigms (yielding 12 total conditions for the Gabor patches and 14 total conditions for the Sloan letters). For Experiment 2, there were 7 pedestal luminance values for the steady-pedestal paradigm, and 6 pedestal luminance values for the pulsed-pedestal paradigm (yielding 13 total conditions for both Gabor patches and Sloan letters). (When the pedestal luminance was equal to the surround, the steady- and pulsed-pedestal paradigms were identical.) For Experiment 3, 6 peak spatial frequencies for the filtered letters were presented under the steady- and pulsed-pedestal paradigms (yielding 12 conditions). The order of test conditions was randomized within each session.

Threshold was measured using an adaptive staircase procedure following rules for accelerated stochastic approximation (Treutwein, 1995). The staircase steps were defined by the relationship

$$X_{n+1} = X_n - \frac{c}{2 + m_{\text{shift}}}(Z_n - \varphi), \quad n > 2, \tag{4}$$

where X_n is the step size on trial n, c is the initial contrast value, m_{shift} is the cumulative number of reversals, Z_n is the observer's response (0 or 1), and φ is the targeted percent correct value, which was 80%. The criterion to complete the staircase was 25 reversals. The threshold for a given staircase was defined as the mean of the contrast values at all staircase steps following the 20th reversal. Data points in the figures represent the means of three staircase threshold estimates, obtained in separate sessions. Error bars indicate one standard error of the mean (SEM).

The number of alternatives differed for letters and Gabor patches (10 letters vs. 2 orientations). The staircase rule converges on the same percent correct value regardless of the number of alternatives, but the different number of alternatives affects the level of chance performance and hence can alter the shape of the psychometric function. Thus, a given percent correct value may lead to a different threshold value depending on the number of alternatives. However, the focus of the present study was the shape of the CSF, not absolute contrast sensitivities. Further, in pilot testing with Sloan letter pairs that included O vs. C and N vs. Z, the same pattern of results was obtained as for the full set of 10 letters. Therefore, the different numbers of alternatives had no effect on the overall conclusions of the study.

3. Results

3.1. Experiment 1: Contrast sensitivity for Sloan letters and Gabor patches

The purpose of Experiment 1 was to evaluate the equivalence of the CSFs for Sloan letters and Gabor patches under conditions that favored either the MC or the PC pathway. The CSFs for Gabor patches are presented in Fig. 3 for subjects S1 (top), S2 (middle), and S3 (bottom). The CSF for the steady-pedestal paradigm (filled squares) was more low-pass than that for the pulsed-pedestal paradigm (filled triangles). As a consequence, the CSFs for the two testing paradigms were well separated at low spatial frequencies and converged at high spatial frequencies. These results for Gabor patches are similar to those of previous studies that used D6 patterns as test stimuli (Alexander, Barnes, Fishman, Pokorny, & Smith, 2004; Leonova et al., 2003). As in a previous study (Leonova et al., 2003), we interpret the results at low spatial frequencies as representing the response of the MC pathway for the steady-pedestal paradigm, and of the PC pathway for the pulsed-pedestal paradigm. At high spatial frequencies, where the functions converge, it is assumed that the PC pathway mediated contrast sensitivity for both paradigms (Leonova et al., 2003).

The curves in Fig. 3 are the least-squares best fits of the log form of an equation that has been used previously to describe the CSF (Rohaly & Owsley, 1993)

$$s = Af^n e^{-pf}, \tag{5}$$

where s is the contrast sensitivity at spatial frequency f, n governs the attenuation at low spatial frequencies, and A and p are vertical and horizontal scaling parameters, respectively, on logarithmic coordinates. A, n, and p were free parameters, and the data were fit using a Marquardt–Levenberg algorithm. These curves provide a satisfactory description of the contrast sensitivity functions for the Gabor patches.

The CSFs for Sloan letters are presented in Fig. 4 for subjects S1 (top), S2 (middle), and S3 (bottom). In Fig. 4, log contrast sensitivity is plotted with respect to the log of the reciprocal of MAR in order to generate CSFs of the same orientation as those for the Gabor patches. The curves in Fig. 4 are the best fits of Eq. (5), with $1/MAR$ substituted for f. Unlike the results for the Gabor patches (Fig. 3), the Sloan letter CSFs for the steady- and pulsed-pedestal paradigms showed a relatively constant separation of approximately 0.4 log units before converging at high spatial frequencies.

A direct comparison of the CSFs for Sloan letters and Gabor patches is presented in Fig. 5 for subjects S1 (top), S2 (middle), and S3 (bottom). The x-axes for letters (upper axis) and Gabor patches (lower axis) were equated as described in Section 2.3. These plots illustrate the marked differences in the shapes of the CSFs for these two types of stimuli. For spatial fre-

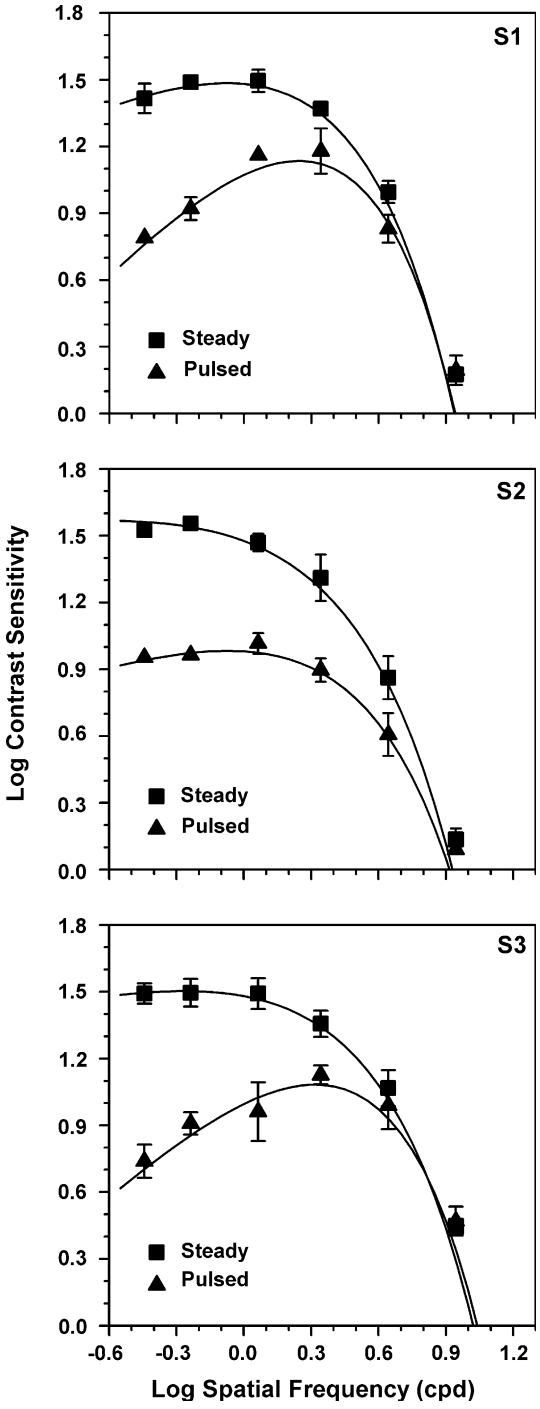

Fig. 3. Log contrast sensitivity as a function of log spatial frequency obtained with Gabor patches for S1, (top), S2 (middle), and S3 (bottom) using the steady-pedestal (filled squares) and pulsed-pedestal (filled triangles) paradigms. Data points represent the means of three threshold estimates; error bars indicate ±1 SEM. The curves represent the least-squares best fits of Eq. (5).

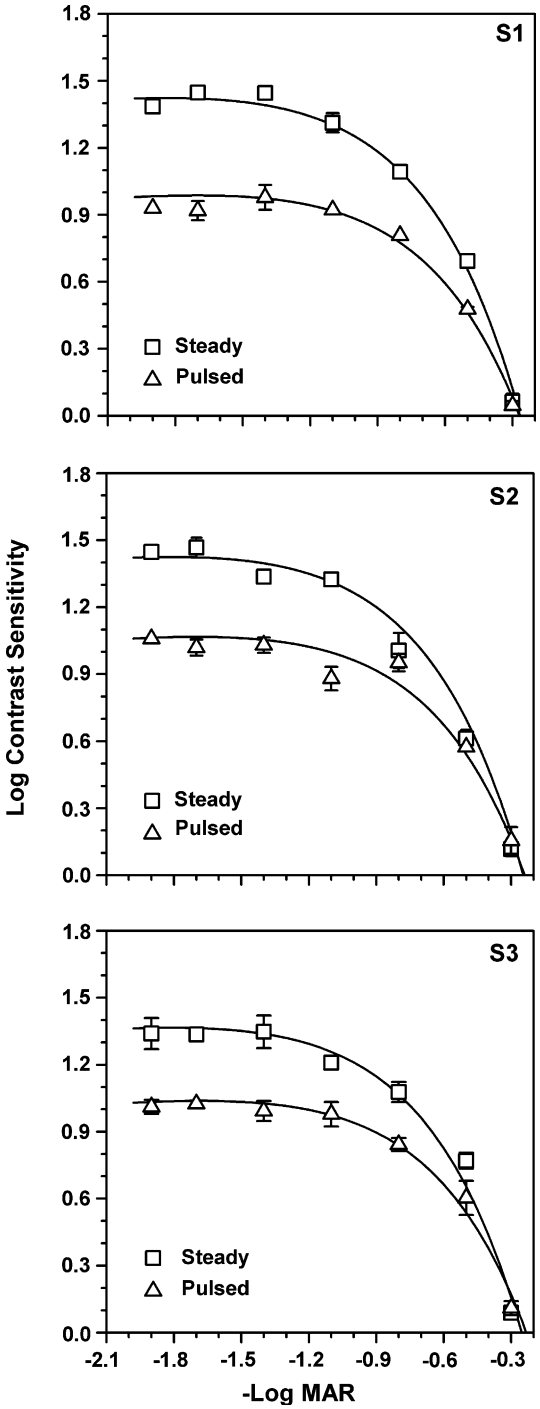

Fig. 4. Log contrast sensitivity as a function of the log of the reciprocal of MAR obtained with Sloan letters for S1, (top), S2 (middle), and S3 (bottom) for the steady-pedestal (unfilled squares) and pulsed-pedestal (unfilled triangles) paradigms. Data points represent the means of three threshold estimates; error bars indicate ±1 SEM. The curves represent the least-squares best fits of Eq. (5).

quencies higher than approximately 0.6 log cpd (letter sizes smaller than 0.9 log MAR, or 20/160 Snellen equivalent), contrast sensitivity was substantially greater for letters than for Gabor patches. At low spatial frequencies (large letter sizes), the CSFs for letters showed a constant separation that was not observed for Gabor patches. Thus, the shape differences between the CSFs for letters and Gabor patches were most pronounced for the pulsed-pedestal paradigm (inferred PC-pathway mediation).

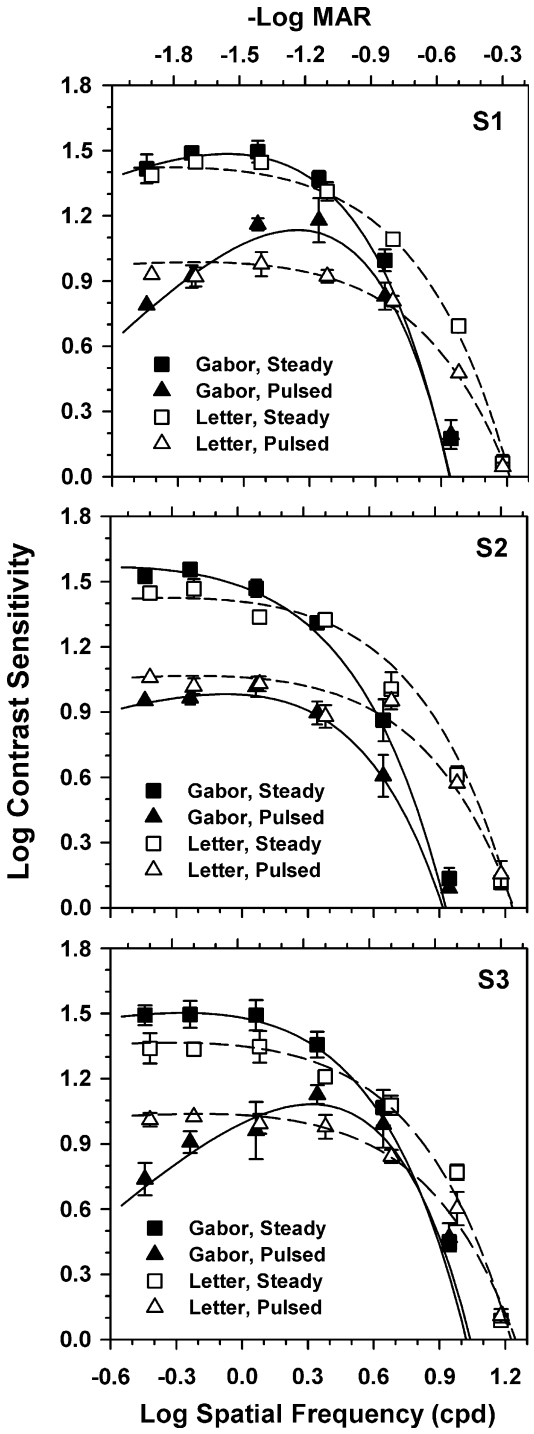

Fig. 5. CSFs for Gabor patches and Sloan letters replotted from Figs. 3 and 4, respectively. The CSFs for Gabor patches are plotted relative to the lower *x*-axis, and the CSFs for Sloan letters are plotted relative to the upper *x*-axis, with the axes equated as described in the text.

3.2. Experiment 2: Increment threshold functions for Sloan letters and Gabor patches

Because the CSFs for Sloan letters were quite similar in shape for the steady- and pulsed-pedestal paradigms at low spatial frequencies (Fig. 4), it is not immediately apparent whether contrast sensitivity was mediated by different visual pathways for the two paradigms, as is presumed to be the case for grating stimuli (Leonova et al., 2003). Experiment 2 addressed this issue by measuring increment thresholds (defined as $[L_t - L_p]$ for Gabor patches and $[L_{max} - L_p]$ for letters) as a function of pedestal luminance, using the steady- and pulsed-pedestal paradigms. In a previous study that used D6 patterns as test stimuli (Leonova et al., 2003), increment threshold functions were markedly different for these two paradigms. For the steady-pedestal paradigm, there was a linear increase in log increment threshold as a function of log pedestal luminance, whereas for the pulsed-pedestal paradigm, the increment threshold function showed a V-shaped pattern.

Experiment 2 employed Sloan letters of an intermediate size (1.4 log MAR) and a Gabor patch with a corresponding spatial frequency (0.1 log cpd). Fig. 6 plots log increment threshold for the Gabor patches as a function of log pedestal luminance for subjects S1 (left) and S2 (right). For the steady-pedestal paradigm (squares), the log increment threshold for Gabor patches increased linearly as log pedestal luminance increased. The least-squares regression lines fit to the steady-pedestal increment thresholds had slopes of 0.78 (S1) and 0.97 (S2). These slopes are consistent with those of Leonova et al. (2003) for a similar spatial frequency. For the pulsed-pedestal paradigm (triangles), the increment threshold for the Gabor patches increased as pedestal luminance was either increased or decreased from the surround luminance, so that the threshold function formed a V-shaped pattern, consistent with the results of Leonova et al. (2003).

The curves fit to the pulsed-pedestal data are the least-squares best fits of Eq. (3) from Pokorny and Smith (1997):

$$\Delta C = K(10/R_{max})(C_{sat} + C)^2/[C_{sat} - (10/R_{max})(C_{sat} + C)], \quad (6)$$

where ΔC is the contrast discrimination threshold, K is a vertical scaling parameter, R_{max} is maximal response amplitude; C_{sat} is a semi-saturation parameter (the contrast at which the response amplitude is half R_{max}), and C is Weber contrast. As in Pokorny and Smith (1997), C_{sat} was set to unity, R_{max} and K were free parameters in the fit, and luminance difference thresholds rather than values of ΔC were plotted. The data for positive and negative pedestal contrasts were fit simultaneously. These curves provide a reasonable fit to the threshold data for the Gabor patches.

Fig. 7 presents log increment thresholds for Sloan letters as a function of log pedestal luminance for subjects S1 (left) and S2 (right). Overall, the pattern of results obtained with the Sloan letter set was similar to the results obtained with Gabor patches. For the steady-pedestal paradigm (open squares), the log increment threshold increased linearly as log pedestal luminance increased, although the slopes of the best-fit regression lines were lower for letters than for Gabor patches (0.52 vs. 0.78 and 0.56 vs. 0.97 for subjects S1 and S2, respectively). A likely explanation for the

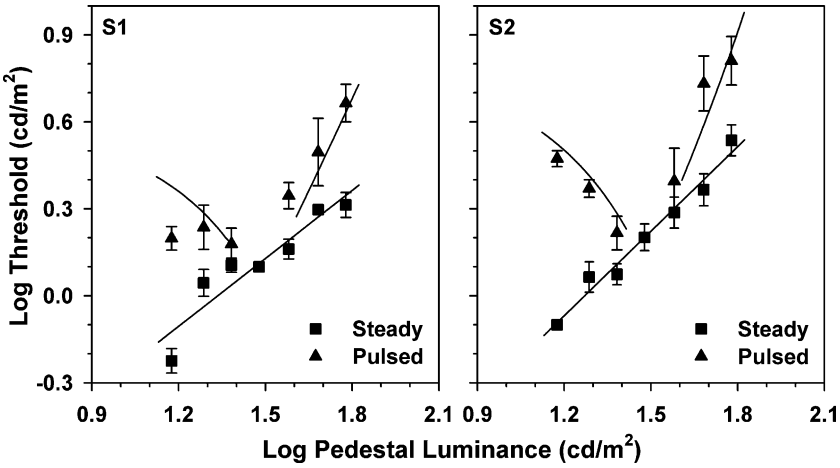

Fig. 6. Log increment threshold as a function of log pedestal luminance for S1 (left) and S2 (right), using Gabor patches that had a spatial frequency of 0.1 log cpd. Data for the steady-pedestal paradigm were fit with a least-squares regression line; data for the pulsed-pedestal paradigm were fit with Eq. (6).

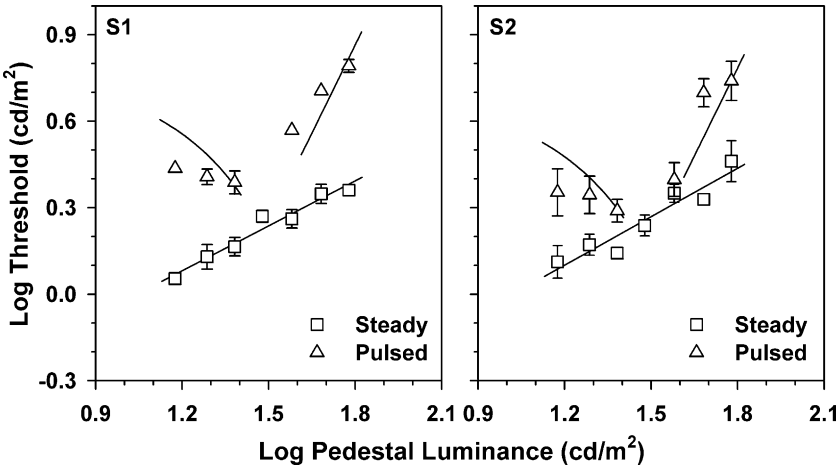

Fig. 7. Log increment threshold as a function of log pedestal luminance for S1 (left) and S2 (right), using Sloan letters that had a log MAR value of 1.4. Data for the steady-pedestal paradigm were fit with a least-squares regression line; data for the pulsed-pedestal paradigm were fit with Eq. (6).

decreased slope for letters is presented in Section 4. For the pulsed-pedestal paradigm (open triangles), the increment threshold increased as the pedestal luminance was either increased or decreased from the surround luminance, forming a V-shaped pattern. As in Fig. 6, the curves fit to the pulsed-pedestal data in Fig. 7 represent the least-squares bests fit of Eq. (6). These curves provide a satisfactory fit to the increment thresholds for the pulsed-pedestal paradigm for letter optotypes. Thus, the results of Experiment 2 are consistent with the hypothesis that letter contrast sensitivity was mediated by two different visual mechanisms, the MC and PC pathways, at this intermediate letter size.

3.3. Experiment 3: Contrast sensitivity for spatially filtered Sloan letters

The results of Experiment 1 demonstrated that the CSFs for Sloan letters and Gabor patches were considerably different in shape and extent. Experiment 2 confirmed that, despite the differences between the CSFs for letters and Gabor patches, increment thresholds for both stimulus types showed properties that were consistent with mediation by the MC and PC pathway for the steady- and pulsed-pedestal paradigms, respectively. The aim of Experiment 3 was to determine whether the observed differences between the shapes of the CSFs for Sloan letters and Gabor patches were due to the broader spatial frequency content of the letters. To examine this possibility, the Sloan letter set was restricted in spatial frequency by using a cosine log filter (Peli, 1990).

The CSFs for spatially filtered Sloan letters are presented in Fig. 8 for subjects S1 (top), S2 (middle), and S3 (bottom). The curves are the least-squares best fits of Eq. (5). The CSFs for filtered letters obtained with the steady-pedestal paradigm (half-filled squares) and pulsed-pedestal paradigm (half-filled diamonds) were well separated at low spatial frequencies and converged at high spatial frequencies, similar to the results obtained with Gabor patches (Fig. 3).

A direct comparison of the CSFs for filtered Sloan letters and Gabor patches is presented in Fig. 9 for subjects

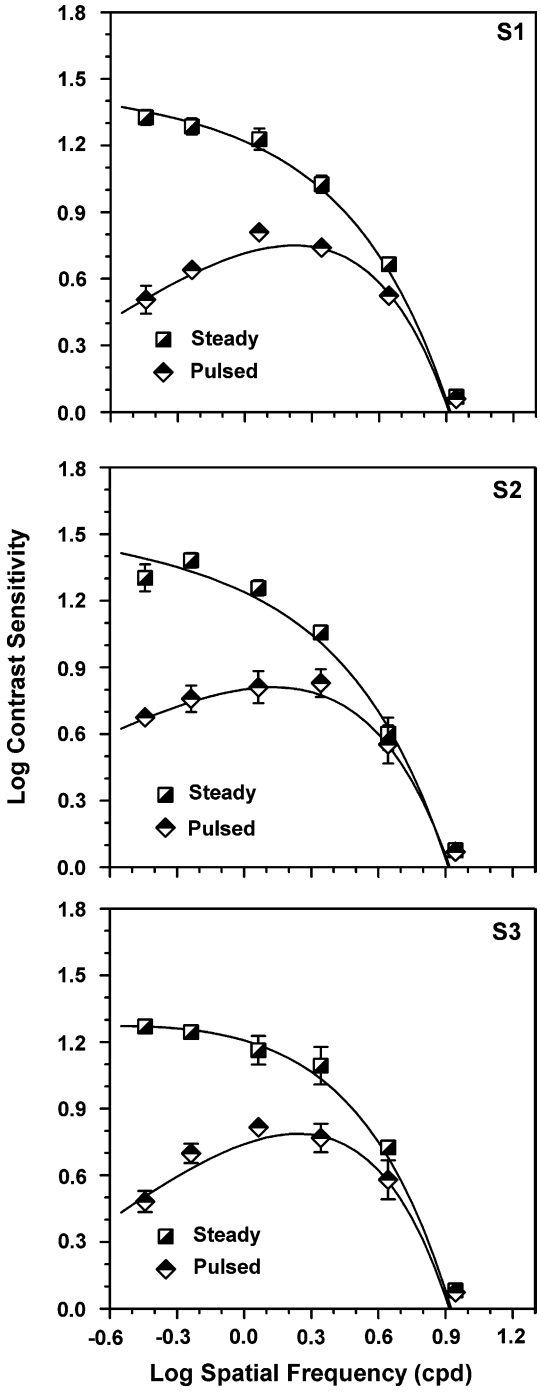

Fig. 8. Log contrast sensitivity as a function of log spatial frequency obtained with spatially filtered Sloan letters for S1, (top), S2 (middle), and S3 (bottom) using the steady-pedestal (squares) and pulsed-pedestal (diamonds) paradigms. Data points represent the means of three threshold estimates; error bars indicate ±1 SEM. The curves represent the least-squares best fits of Eq. (5).

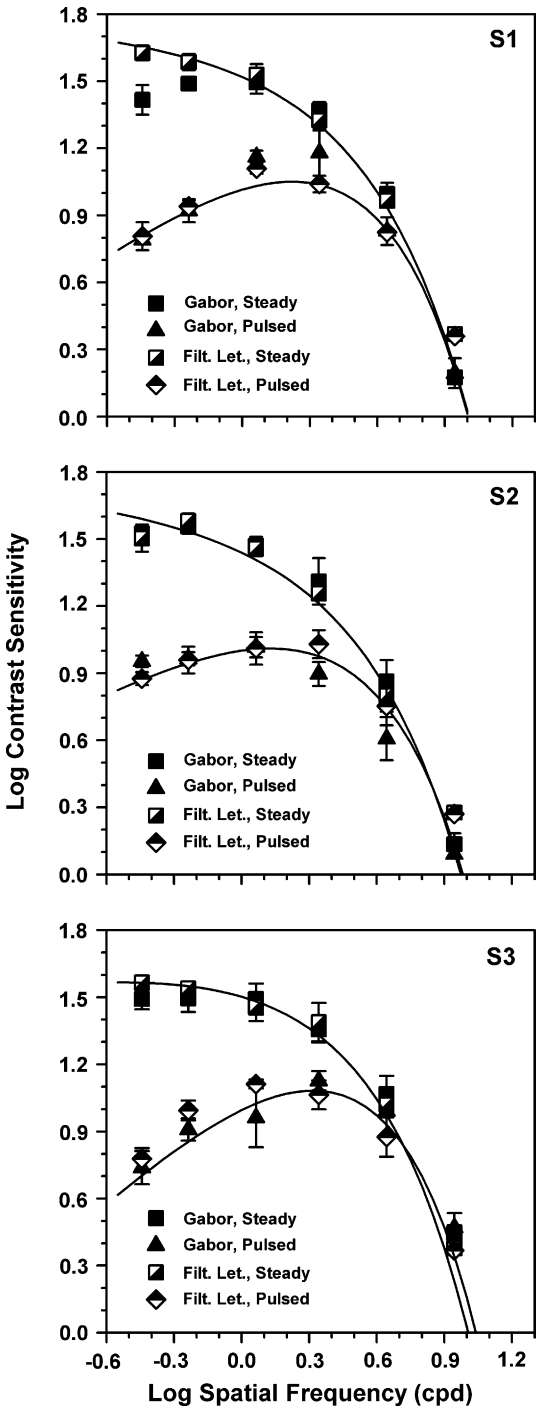

Fig. 9. CSFs for Gabor patches and filtered Sloan letters replotted from Figs. 3 and 8, respectively. The data sets for the filtered letters were shifted vertically (see text for details). The curves represent the least-squares best fits of Eq. (5) to the data for the filtered letters.

S1 (top) S2 (middle), and S3 (bottom). In Fig. 9, the data for the Gabor patches have been replotted from Fig. 3. The data for the filtered letters have been replotted from Fig. 8, but have been shifted uniformly upwards for each subject by the mean difference in sensitivity between the filtered letters and Gabor patches (0.26, 0.17, and 0.30 log units for subjects S1, S2, and S3, respectively). It is apparent from Fig. 9 that the CSFs for the filtered Sloan letters and Gabor patches were quite similar in shape. Thus, the differences in the shapes of the CSFs for standard letters and Gabor patches, evident in Fig. 5, are due to the broad spatial frequency content of the unfiltered Sloan letters.

4. Discussion

The aim of this study was to determine whether letter optotypes and grating stimuli provide equivalent information about contrast sensitivity under testing conditions designed to favor either the MC or PC pathway. The results indicate that there are systematic differences between the CSFs obtained with these two types of test stimuli. For Gabor patches, the CSFs for the steady- and pulsed-pedestal paradigms diverged at low spatial frequencies (Fig. 3), confirming previous studies (Alexander et al., 2004; Leonova et al., 2003). In comparison, the CSFs for letters showed a constant separation at low spatial frequencies for the steady- and pulsed-pedestal paradigms (Fig. 4). Further, there was a substantially higher sensitivity for small letters than for Gabor patches of equivalent nominal spatial frequencies (Fig. 5).

Despite the marked differences between the shapes of the CSFs for letter optotypes and Gabor patches, the increment threshold functions for the two types of test stimuli showed similar trends (Figs. 6 and 7). For both types of test stimuli, the results for the steady-pedestal paradigm showed a monotonically increasing log increment threshold as a function of log pedestal luminance, consistent with mediation by the MC pathway. For the pulsed-pedestal paradigm, the increment threshold functions for both types of test stimuli showed a V-shaped pattern as a function of log pedestal luminance, consistent with mediation by the PC pathway (Leonova et al., 2003). Therefore, despite the differences in the shapes of the CSFs for letters and Gabor patches at low spatial frequencies, Experiment 2 supported the hypothesis that contrast sensitivities were mediated by MC and PC pathways, respectively, for the steady- and pulsed-pedestal paradigms for both types of test stimulus.

When the Sloan letters were restricted in frequency content through spatial band-pass filtering, the resulting CSFs were identical in shape to those for Gabor patches for both the steady- and pulsed-pedestal paradigms (Fig. 9). Thus, the differences in the shapes of the CSFs for standard Sloan letters and Gabor patches observed in Fig. 5 can be attributed to the broad frequency content of the letters. A similar conclusion was reached in a previous study that did not explicitly target the MC and PC pathways (Alexander et al., 1994). Although the shapes of the CSFs were similar for filtered letters and Gabor patches, a vertical scaling factor was necessary to align the CSFs. This is most likely due to the relative contrast definition that was used for the filtered letters, which was based on the contrast of the unfiltered letters from which they were derived. An additional consideration is that letter identification is likely based on more than a single one-octave band of object frequencies (Gold, Bennett, & Sekuler, 1999), so that restricting the spatial frequency content of letters to one octave would likely reduce contrast sensitivity relative to the letters from which they were derived.

The availability of multiple object frequencies as a basis for letter identification likely accounts for the parallel shapes of the letter CSFs for the steady- and pulsed-pedestal paradigms at intermediate to large letter sizes (Fig. 4). Initially, it was generally assumed that letter identification is scale invariant: that identification is based on a constant band of object frequencies (cpl) regardless of letter angular subtense. However, subsequent studies have shown that the object frequencies that govern letter identification vary systematically with letter angular subtense (Alexander et al., 1994; Chung et al., 2002; Majaj et al., 2002). As a consequence, the retinal spatial frequency (cpd) used for letter identification does not shift in direct proportion to letter angular subtense. Therefore, for intermediate to large letter sizes, it is likely that approximately the same band of retinal spatial frequencies was tested repeatedly in our study despite the change in letter visual angle, thus accounting for the relatively constant separation between the letter CSFs for the steady- and pulsed-pedestal paradigms (Fig. 4).

The broad frequency content of letters also likely accounts for the higher contrast sensitivities for standard Sloan letters at small letter sizes than for Gabor patches of equivalent nominal spatial frequencies (Fig. 5). That is, as letter size approaches the acuity limit, the higher object frequencies contained within the letters exceed the resolution limit, and identification becomes based on lower object frequencies (Alexander et al., 1994; Majaj et al., 2002). Thus, a relatively good level of contrast sensitivity is maintained despite the decreasing letter size.

For the steady-pedestal paradigm, the slope of the increment threshold function was lower for letters (Fig. 7) than for Gabor patches (Fig. 6) of an intermediate size (spatial frequency). A shallow slope of the increment threshold function has also been observed for grating stimuli when the spatial frequency is relatively high (Leonova et al., 2003). In our study, letter optotypes and Gabor patches were equated nominally in terms of spatial frequency, using the conventional assumption that a letter with a log MAR value of 0.0 (stroke width of 1 arcmin; object frequency of 2.5 cpl) corresponds to a spatial frequency of 30 cpd. However, the relatively shallow slope of the increment threshold function for Sloan letters (Fig. 7) suggests that letter identification was based on object frequencies higher than 2.5 cpl (i.e., higher retinal spatial frequencies than the nominal 1.25 cpd).

In conclusion, our results indicate that letter optotypes and grating stimuli do not necessarily provide equivalent information about contrast sensitivity, particularly under test conditions that emphasize the PC pathway. Therefore, the use of letter optotypes, with their broad spatial frequency content, can potentially complicate the interpretation of contrast sensitivity deficits in ocular diseases. For example, patients with X-linked retinoschisis, a form of early-onset macular degeneration in males, can have normal letter contrast sensitivity using the Pelli–Robson letter contrast sensitivity chart but reduced contrast sensitivity for grating stimuli of the same nominal spatial frequency (Alexander, Barnes, & Fishman, 2005), a discrepancy that is likely

due to the broad frequency content of letter optotypes. Spatially band-pass filtered letters, in combination with the use of steady- and pulsed-pedestal paradigms, could potentially alleviate some of the difficulty in interpreting the contrast sensitivity deficits of patients with eye disease while maintaining some of the advantages of letters.

Acknowledgments

This research was supported by NIH research grant EY08301, NIH core grant EY01792, and an unrestricted departmental grant from Research to Prevent Blindness. KRA is a Research to Prevent Blindness Senior Scientific Investigator. We thank Boaz Super for assistance in implementing the cosine log filter, and Aparna Raghuram for serving as a subject.

References

Alexander, K. R., Barnes, C. S., & Fishman, G. A. (2005). Characteristics of contrast processing deficits in X-linked retinoschisis. *Vision Research, 45*, 2095–2107.

Alexander, K. R., Barnes, C. S., Fishman, G. A., Pokorny, J., & Smith, V. C. (2004). Contrast sensitivity deficits in inferred magnocellular and parvocellular pathways in retinitis pigmentosa. *Investigative Ophthalmology and Visual Science, 45*, 4510–4519.

Alexander, K. R., Derlacki, D. J., & Fishman, G. A. (1992). Contrast thresholds for letter identification in retinitis pigmentosa. *Investigative Ophthalmology and Visual Science, 33*, 1846–1852.

Alexander, K. R., Derlacki, D. J., Fishman, G. A., & Szlyk, J. P. (1993). Temporal properties of letter identification in retinitis pigmentosa. *Journal of the Optical Society of America A, 10*, 1631–1636.

Alexander, K. R., Xie, W., & Derlacki, D. (1993). The effect of contrast polarity on letter identification. *Vision Research, 33*, 2491–2497.

Alexander, K. R., Xie, W., & Derlacki, D. (1994). Spatial-frequency characteristics of letter identification. *Journal of the Optical Society of America A, 11*, 2375–2382.

Brainard, D. (1997). The psychophysics toolbox. *Spatial Vision, 10*, 433–436.

Chung, S. T., Legge, G. E., & Tjan, B. S. (2002). Spatial-frequency characteristics of letter identification in central and peripheral vision. *Vision Research, 42*, 2137–2152.

Gold, J. M., Bennett, P. J., & Sekuler, A. B. (1999). Identification of band-pass filtered letters and faces by human and ideal observers. *Vision Research, 39*, 3537–3560.

Graham, N. V. S. (1989). *Visual pattern analyzers*. New York: Oxford University Press.

Herse, P. R., & Bedell, H. E. (1989). Contrast sensitivity for letter and grating targets under various stimulus conditions. *Optometry & Vision Science, 66*, 774–781.

Kaplan, E., Lee, B. B., & Shapley, R. M. (1990). New views of primate retinal function. In N. N. Osborne & G. T. Chader (Eds.), *Progress in retinal research* (pp. 273–336). Oxford: Pergamon Press.

Kulikowski, J. J., & Tolhurst, D. J. (1973). Psychophysical evidence for sustained and transient detectors in human vision. *Journal of Physiology, 232*, 149–162.

Lee, B. B. (1996). Receptive field structure in the primate retina. *Vision Research, 36*, 631–644.

Legge, G. E. (1978). Sustained and transient mechanisms in human vision: Temporal and spatial properties. *Vision Research, 18*, 69–81.

Lennie, P. (1993). Roles of the M and P pathways. In R. Shapley & D. M. K. Lam (Eds.), *Contrast sensitivity* (pp. 201–213). Cambridge, MA: MIT press.

Leonova, A., Pokorny, J., & Smith, V. C. (2003). Spatial frequency processing in inferred PC- and MC-pathways. *Vision Research, 43*, 2133–2139.

Majaj, N. J., Pelli, D. G., Kurshan, P., & Palomares, M. (2002). The role of spatial frequency channels in letter identification. *Vision Research, 42*, 1165–1184.

Merigan, W. H., & Maunsell, J. H. (1993). How parallel are the primate visual pathways. *Annual Review of Neuroscience, 16*, 369–402.

National Academy of Sciences-National Research Council (1980). Recommended and standard procedures for the clinical measurement and specification of visual acuity: Report of working group 39. *Advances in Ophthalmology 41*, 103–148.

Peli, E. (1990). Contrast in complex images. *Journal of the Optical Society of America A, 7*, 2032–2040.

Pelli, D. G., Robson, J. G., & Wilkins, A. J. (1988). The design of a new letter chart for measuring contrast sensitivity. *Clinical Vision Science, 2*, 187–199.

Pokorny, J., & Smith, V. C. (1997). Psychophysical signatures associated with magnocellular and parvocellular pathway contrast gain. *Journal of the Optical Society of America A, 14*, 2477–2486.

Regan, D. (1991). Do letter charts measure contrast sensitivity? *Clinical Vision Science, 6*, 401–408.

Regan, D., Raymond, J., Ginsburg, A. P., & Murray, T. J. (1981). Contrast sensitivity, visual acuity and the discrimination of Snellen letters in multiple sclerosis. *Brain, 104*, 333–350.

Rohaly, A. M., & Owsley, C. (1993). Modeling the contrast-sensitivity functions of older adults. *Journal of the Optical Society of America A, 10*, 1591–1599.

Swanson, W. H., & Wilson, H. R. (1985). Eccentricity dependence of contrast matching and oblique masking. *Vision Research, 25*, 1285–1295.

Treutwein, B. (1995). Adaptive psychophysical procedures. *Vision Research, 35*, 2503–2522.

Wang, Y. Z., Bradley, A., & Thibos, L. N. (1997). Aliased frequencies enable the discrimination of compound gratings in peripheral vision. *Vision Research, 37*, 283–290.

Wilson, H. R. (1980). Spatiotemporal characterization of a transient mechanism in the human visual system. *Vision Research, 20*, 443–452.